Correlation Length and Entanglement Spacing in Concentrated Hydrogenated Polybutadiene Solutions

Hui Tao,[†] Ching-i Huang,[‡] and Timothy P. Lodge*,[†]

Department of Chemistry and Department of Chemical Engineering & Materials Science, University of Minnesota, Minneapolis, Minnesota 55455-0431

Received September 16, 1998; Revised Manuscript Received December 28, 1998

ABSTRACT: The concentration correlation length, ξ, and the entanglement spacing, d, have been determined in solutions of hydrogenated polybutadiene in *n*-alkane solvents at 140 °C by small-angle neutron scattering and rheology, respectively. The former varies as $\xi \sim \phi^{-0.76}$ over the range $0.04 < \phi < 0.7$. This result is in agreement with scaling predictions for semidilute solutions in a good solvent, but interestingly this dependence extends to concentrations well beyond the regime where the scaling law should be valid. The entanglement spacing was obtained via measurements of the dynamic loss modulus, G'', as a function of frequency, ω, from $\phi = 0.2$ to $\phi = 1$. The maximum value of G'' in the terminal dispersion regime varies as $\phi^{1.9}$, implying that $d \sim \phi^{-0.45}$. The shape of $G''(\omega)$ was independent of ϕ and M, and d was independent of M, as expected for well-entangled solutions. These results indicate that the entanglement spacing and the correlation length need not have the same concentration dependence in concentrated solutions in a good solvent. The ratio ξ/d, termed the constraint porosity parameter in the polymer mode-coupling theory, varies from 0.09 in the melt to 0.15 when $\phi = 0.2$, which may have important implications for the concentration dependence of the molecular weight exponent for chain diffusion.

Introduction

The structure and dynamics of concentrated homopolymer solutions remain incompletely characterized or understood. The linear viscoelastic properties of such solutions have been examined extensively over the past four decades, but with the advent of the reptation model,[1] experimental efforts tended to focus either on melts or on semidilute solutions, where simple scaling law concentration dependences have been proposed;[2,3] the intervening concentration regime has received less attention. One major advance that can be directly attributed to the reptation hypothesis is the realization that chain diffusion and rheology are intimately connected; this connection had been largely dormant since the early work of Bueche.[4] As a result, there have been many studies of polymer diffusion in the melt and in semidilute solution over the past two decades,[3,5] but only a single series of measurements have been reported on concentrated solutions (i.e., for concentrations between 20% and 100%).[6−8] Similarly, despite their central importance, the structure factor for concentrated solutions, and the corresponding static screening length, have only been examined up to concentrations near 30%.[9,10]

The original reptation-plus-scaling approach to semidilute solutions assumed a single important length scale intermediate between the Kuhn length and the radius of gyration, namely the screening length ξ.[2] However, it has since become abundantly clear that this screening length and the entanglement length scale, d (or tube diameter in the reptation framework), are distinct and can have different dependences on concentration. These dual length scales have been carefully incorporated into the reptation-plus-scaling approach by Colby and co-workers,[11−13] but the distinction between ξ and d is not dependent on the assumption of reptation. For example, the polymer mode-coupling theory of Schweizer and co-workers recognizes a logical distinction between the equilibrium pair distribution of polymer segments and the dynamic correlations among chains.[14−16] Consequently, in order that experimental measurements of polymer dynamic properties be fairly compared with recent theories, it is important to characterize both ξ and d. To this end we report measurements of ξ (by SANS) and d (from rheology) on solutions of hydrogenated polybutadienes in *n*-alkane solvents, over the concentration range from 20% to the melt. Extensive measurements of the diffusivity and viscosity in the same system will be described subsequently.[17,18]

Experimental Section

Samples and Solutions. Four hydrogenated (deuterated) polybutadienes h(d)PB were employed. They were prepared by living anionic polymerization of 1,3-butadiene in cyclohexane at 40 °C, using *sec*-butyllithium as the initiator, followed by hydrogenation (or deuteration) in a high-pressure reactor using $Pd/CaCO_3$ as the catalyst. The molecular weights and polydispersities of the polymers were determined by size exclusion chromatography in four different modes. The PB precursors were examined against a calibration based on PB standards and also utilizing a multiangle light scattering detector (Wyatt DAWN) to ascertain the molecular weights directly. Then, the h(d)PB samples were analyzed at high temperature, and the molecular weights were determined by universal calibration against polystyrene standards. These three methods gave generally consistent results, which were then averaged ("set A"). Finally, the h(d)PB samples were analyzed on a high-temperature instrument (Polymer Labs 210) equipped with a Wyatt DAWN detector at the E.I. DuPont de Nemours and Company Central Research and Development Laboratory by Dr. P. M. Cotts. These results ("set B") were deemed the most reliable, in that the light scattering detection removed the need for column calibration, and the high-temperature capability permitted direct analysis of the satu-

* Author for correspondence.
[†] Department of Chemistry.
[‡] Department of Chemical Engineering & Materials Science.

10.1021/ma981468d CCC: $18.00
Published on Web 01/28/1999

rated products. "Set B" values agreed with "set A" to within 10%, and consequently we take the final values as the average of these two sets. Polydispersities are taken entirely from "set B", due to the relative insensitivity of the light scattering detection to band broadening. The samples are designated hPB-50, with $M_w = 5.3_2 \times 10^4$ and $M_w/M_n \approx 1.003$; hPB-200, with $M_w = 1.9_4 \times 10^5$ and $M_w/M_n \approx 1.01$; dPB-200, with $M_w = 2.0_3 \times 10^5$ and $M_w/M_n \approx 1.01$; hPB-350, with $M_w = 3.5_0 \times 10^5$ and $M_w/M_n \approx 1.03$; dPB-350, with $M_w = 3.6_4 \times 10^5$ and $M_w/M_n \approx 1.03$; and dPB-440, with $M_w = 4.4_0 \times 10^5$ and $M_w/M_n \approx 1.04$.

The microstructure of the polybutadienes and the degree of saturation were assessed by ^{1}H NMR. The former ranged from 7.3% 1,2-addition for hPB-50 to 4.2% for dPB-440, and the latter was consistently >99%. Consequently, these polymers may be viewed as random copolymers of ethylene and 1-butene, with 1.9 to 1.1 ethyl branches per 100 backbone carbons; they would be designated PEB-2 or PEB-1 in the nomenclature employed in some references.[19] Deuteration introduced ca. three deuterons per repeat unit, due to exchange. Linear alkane solvents were obtained from Aldrich ($C_{24}H_{50}$) and CDN Isotopes ($C_{16}D_{34}$). Solutions were prepared gravimetrically, using toluene as a cosolvent, followed by annealing above the melting temperature of h(d)PB (ca. 110−120 °C). A small quantity (<0.5%) of antioxidant (BHT) was added to each sample. Concentrations are reported as volume fraction polymer, ϕ, assuming additivity of volumes and densities at 140 °C of 0.782_9, 0.724_4, and 0.795_6 g/mL for hPB,[20] $C_{24}H_{50}$, and $C_{16}D_{34}$,[21] respectively. SANS samples were sealed in homemade cells fashioned from quartz disks, with a path length of 1.0 mm. The SANS measurements utilized hPB-50 and $C_{16}D_{34}$ exclusively. This polymer was selected to be of sufficiently high molecular weight that a reasonable semidilute regime could be accessed, but not so high that specimen preparation was too tedious.

Small-Angle Neutron Scattering. SANS measurements were performed at the National Institute of Standards and Technology Cold Neutron Research Facility on the NIST/Exxon/University of Minnesota 30 m instrument (NG-7). Neutrons with $\lambda = 6.0$ Å and $\Delta\lambda/\lambda = 0.10$ were incident on samples maintained at 140 ± 0.2 °C in a temperature-controlled block. The detector was placed 3.0 m behind the sample, with center offset by 15 cm, to provide a usable q range of ca. 0.02−0.2 Å^{-1}. Scattering data were corrected for detector sensitivity, background, empty cell scattering, and transmission factors, azimuthally averaged, and then placed on an absolute scale ($d\Sigma/d\Omega$) using a silica standard (A5). Incoherent scattering contributions were estimated utilizing measurements on the pure solvent and hPB and were typically in the range 0.1−0.8 cm^{-1}.

Rheology. Measurements of the dynamic shear moduli, G' and G'', were performed on a Rheometric Scientific DSR in the parallel plate geometry at 140 ± 1 °C. Upper plates (8 mm diameter) with serrated surfaces were employed to reduce sample slip, and the typical gap thickness was 0.8−1.3 mm. Strain amplitudes of 0.03−0.08 were sufficiently small to ensure linear response. The measurements were corrected for the error in the torque measurement due to sample protrusion from the gap, following standard procedures.[22] Solutions of h(d)PB-200, h(d)PB-350, and dPB-440 in $C_{24}H_{50}$, with concentrations ranging from $\phi = 0.2$ to 1.0, were examined. It is assumed henceforth that the rheological properties of a given solution are independent of whether the particular polymer was hydrogenated or deuterated.

Results

The static screening length, ξ, may be defined by the Ornstein−Zernike equation:

$$I_{coh}(q) = \frac{I(0)}{1 + q^2\xi^2} \tag{1}$$

where I_{coh} refers to the absolute coherent scattered intensity and q is the scattering vector. The scattering

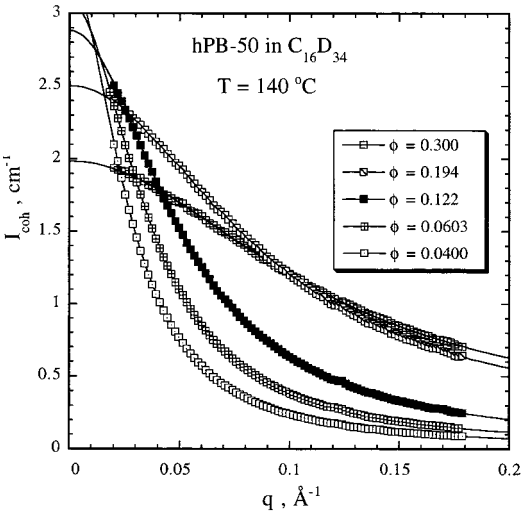

Figure 1. Absolute coherent scattered intensity versus wavevector for the indicated concentrations; smooth curves represent fits to the Ornstein−Zernike equation as discussed in the text.

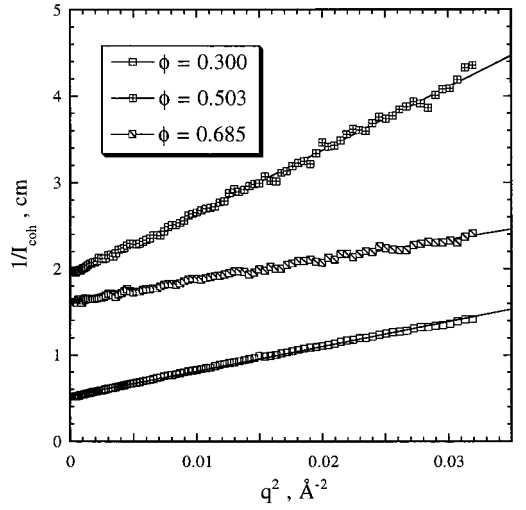

Figure 2. Inverse absolute coherent scattered intensity versus wavevector for the indicated concentrations; the lines indicate linear regression fits.

profiles from solutions with $\phi \leq 0.3$ were fit directly to eq 1 using ξ and $I(0)$ as adjustable parameters but also allowing for a finite baseline due to uncertainty in the incoherent background. The data and the resulting fits are shown in Figure 1; in all cases the fit is clearly excellent. The extra baseline term varied from 0.015 to 0.18 cm^{-1} with increasing concentration in Figure 1, which represents a modest contribution for these solutions. For solutions with $\phi > 0.4$ the change in intensity over the measured q range was significantly weaker, and consequently fits to eq 1 with an adjustable baseline were unreliable. However, by assuming that this term was unnecessary, it was possible to fit I^{-1} versus q^2 to a straight line with comparable success; this is illustrated in Figure 2. The data for $\phi = 0.300$ from Figure 1 are also included, to ensure that the two fitting procedures gave equivalent results. The resulting concentration dependence of ξ is shown in Figure 3, and the data are listed in Table 1. The data were fit to a power law, which yields the expression

$$\xi = \xi_0\phi^{-0.76} \tag{2}$$

with $\xi_0 = 3.29$ Å.

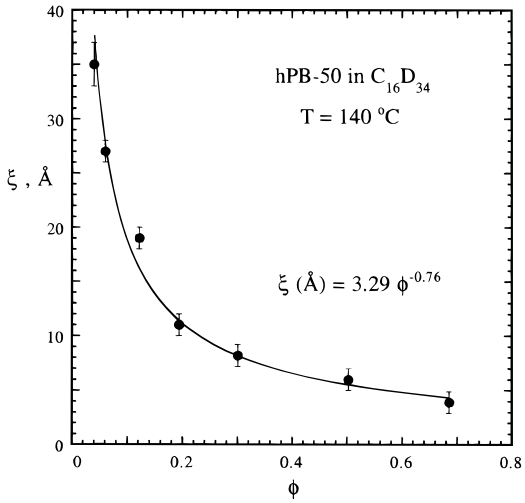

Figure 3. Correlation length versus concentration; the smooth curve represents the fit to a power law.

Table 1. Concentration Correlation Length for hPB-50 in $C_{16}D_{34}$

ϕ	ξ (Å)	ϕ	ξ (Å)
0.0400	35 ± 2	0.300	8.2 ± 1
0.0603	27 ± 1	0.503	6 ± 1
0.122	19 ± 1	0.685	3.9 ± 1
0.194	11 ± 1		

Information about the entanglement length scale may be accessed in a variety of ways, such as through neutron spin-echo measurements of restricted segmental motions.[23] However, the most common approach is through the plateau modulus, G_N, and the entanglement molecular weight, M_e:

$$G_N = \frac{4}{5}\phi \frac{\rho RT}{M_e} \tag{3}$$

where ρ is the bulk polymer density and R is the gas constant.[19,24] The entanglement length, d, is then determined by

$$d^2 = M_e \frac{\langle h^2 \rangle}{M} \tag{4}$$

where $\langle h^2 \rangle$ is the mean-square end-to-end distance of the chain. The concentration dependence of d thus reflects the concentration dependence of G_N (or M_e) and the chain dimensions. Westermann et al. have recently measured the chain dimensions for an hPB with $M = 2.8 \times 10^4$ over the range $0.25 \le \phi \le 1$, in $C_{19}D_{40}$ at 150 °C, with the result that $\langle h^2 \rangle$ is effectively constant over this concentration range.[25] Thus $d \sim \phi^{(1-\alpha)/2}$ when $G_N \sim \phi^\alpha$.

The values of G_N were obtained for several h(d)PB/$C_{24}H_{50}$ solutions at 140 °C by determining the maximum value of $G''(\omega)$ in the crossover from the terminal to the plateau regimes and multiplying by 3.56. This approach was necessitated by the limited accessible frequency range but has been demonstrated to be reliable on many systems.[24,26,27] The crucial assumption in this case is that the shape of the dispersion in $G''(\omega)$ not be a strong function of concentration or molecular weight. The constant 3.56 was determined by Raju et al.[26] by applying the following equation to loss modulus data for various entangled polymers:

$$G_N = G''_m \left(\frac{2}{\pi}\right) \int_{-\infty}^{\infty} \left(\frac{G''(\omega/\omega_m)}{G''_m}\right) \mathrm{d} \ln(\omega/\omega_m) \tag{5}$$

Accordingly, in Figure 4a–c we compare G''/G''_m vs ω/ω_m for various concentrations of h(d)PB-180, h(d)PB-350, and dPB-440, respectively; the subscript m denotes the location of the maximum. In all cases the curves superpose extremely well, indicating that there is no significant change in the shape of the terminal dispersion with concentration. (The possible exception is the lowest concentration solution for the highest molecular weight.) Furthermore, the three different molecular weights superpose with each other equally well, as illustrated for the melts in Figure 5. This superposition, in fact, is rather remarkable, for example in comparison to that obtained by Raju et al.[26] Interestingly, Raju et al. also examined hPB samples and found that they did not fit well with other materials. In particular, the peak in $G''(\omega)$ for hPB was distinctly narrower than the "universal" curve they proposed for other materials. In our case integration according to eq 5 gives a conversion factor of 3.3, slightly lower than 3.56, but not substantially different. The narrowness of the peak is directly correlated to the apparent power law exponent on the high-frequency side of the peak. As shown in Figure 5, this exponent is approximately −0.37, in contrast to the values of −0.23, −0.18, and −0.15 reported for high molecular weight polystyrene,[28] polybutadiene,[28] and poly(vinyl methyl ether).[27] Thus, there is apparently some chemical-structure-specific contribution to the shape of the relaxation spectrum. In Figure 6 the concentration dependence of G''_m is plotted on a double-logarithmic scale. The data (also tabulated in Table 2) show some scatter but are consistent with a power law: $G''_m = 5.9 \times 10^5 \phi^{1.9\pm0.1}$ (Pa). Consequently, the entanglement length scales approximately as $d \sim \phi^{-0.45}$.

Discussion

Static Correlation Length. The observed concentration dependence of ξ is intriguing, in that it appears to match the simple scaling prediction for a semidilute solution in a good solvent (i.e., $\xi \sim \phi^{-3/4}$). This correspondence is probably fortuitous in part, however, in that the assumptions underlying the semidilute scaling relation are clearly violated at such high concentrations (ϕ as large as 0.68). The good solvent character of the *n*-alkanes at 140 °C is established by the intrinsic viscosity/molecular weight relationship: we obtained $[\eta] = 0.0305M^{0.72}$ mL/g, which compares favorably with a much earlier result.[29] This intrinsic viscosity exponent ($=3\nu - 1$) implies that the excluded-volume exponent $\nu = 0.57$, which in turn anticipates $\xi \sim \phi^{-0.80}$. Given the limited number of ξ values that we have obtained in the semidilute regime, these exponents are consistent. Note that ξ is expected to be independent of M in this regime, as has been amply confirmed for polystyrene.[9] The result embodied in eq 2 may also be compared with the extensive results for polystyrene in good solvents as compiled by Brown and Nicolai:[9] ξ (Å) $= 2.6\phi^{-0.72}$. These authors note that this relation applies up to concentrations near 30%, which again exceeds the semidilute regime. (The high concentration limit of the semidilute regime is typically taken as ca. 10%; for good solvent systems the important issue is the neglect of ternary contacts in the scaling analysis.) Furthermore,

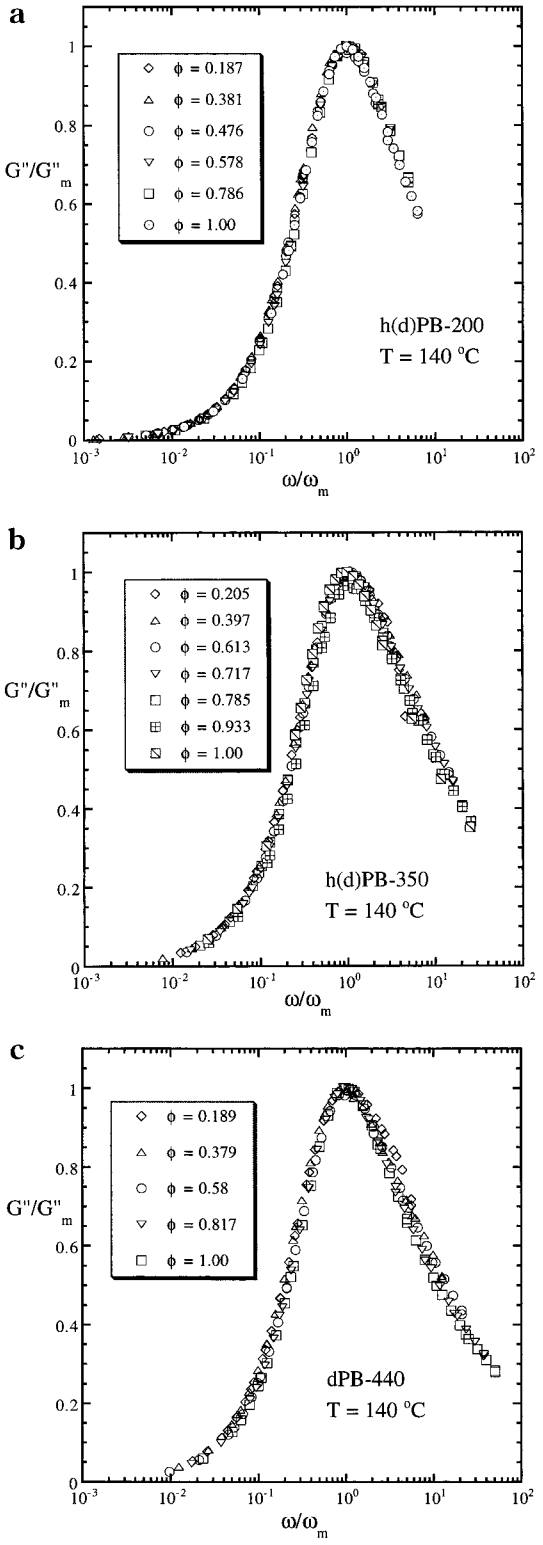

Figure 4. Loss modulus, G'', at 140 °C normalized by its maximum value, G''_m, versus reduced frequency for the indicated concentrations: (a) h(d)PB-200, (b) h(d)PB-350, and (c) dPB-440 in $C_{24}H_{50}$.

the resulting values of ξ at high concentrations lie below the persistence length and thus cannot reasonably be interpreted in terms of the screening of excluded-volume interactions. In the scaling picture, a chain in a good solvent will contract with increasing concentration until the Gaussian (melt) dimensions are achieved. The concentration at which contraction ends can be used to define ϕ^{**}, the onset of the concentrated regime. Wes-

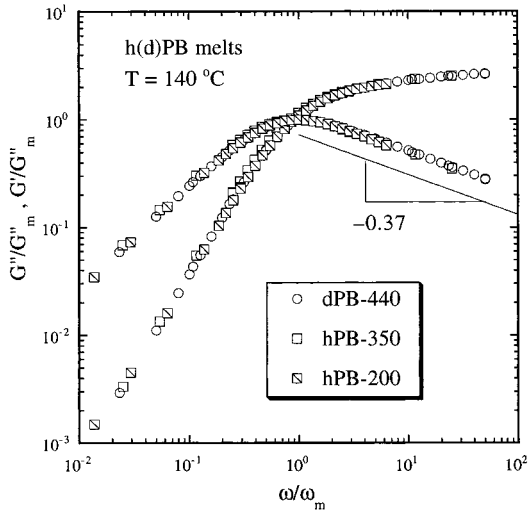

Figure 5. Normalized storage and loss moduli for hPB-200, hPB-350, and dPB-440.

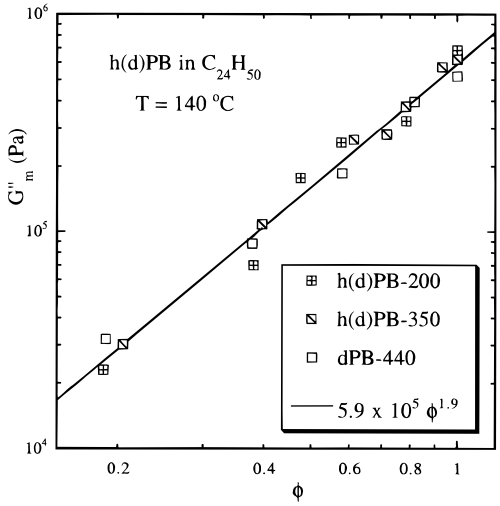

Figure 6. Maximum loss modulus G''_m at 140 °C versus concentration for the indicated molecular weights; the line indicates the fit to a power law.

termann et al.'s results, referred to earlier, imply that $\phi^{**} \leq 0.25$.[25] Our results indicate that, at $\phi = 0.25$, $\xi \approx$ 9.4 Å, which is already comparable to the persistence length. Consequently, although the data for $\xi(\phi)$ apparently follow a single power law over a broad concentration range, the significance of the exponent value changes. At the lower (semidilute) concentrations it reflects the screening of excluded-volume interactions in a good solvent, whereas in the concentrated regime it must reflect the details of interchain packing and chemical structure.[3] A mean-field approach anticipates $\xi \sim \phi^{-1/2}$,[3] whereas others have predicted a crossover to a ϕ-independent correlation length at high concentration.[30]

Entanglement Length. Recently, a great deal of attention has been devoted to the problem of a universal description of the entanglement length and the plateau modulus.[19,23,31] Richter et al. categorize four approaches, which they term scaling models, packing models, binary contact models, and topological models.[23] The relevant results for the ϕ dependence of d and G_N may be summarized as follows:

$$G_N \sim \phi^{\alpha}; \qquad d \sim \phi^{(1-\alpha)/2} \tag{6}$$

Table 2. Maximum Value of G'' (MPa) at 140 °C in $C_{24}H_{50}$

polymer	ϕ	G''_m	polymer	ϕ	G''_m	polymer	ϕ	G''_m
hPB-200	1.00	0.683	hPB-350	1.00	0.619	dPB-440	1.00	0.518
hPB-200	0.786	0.324	dPB-350	0.933	0.571	dPB-440	0.817	0.396
hPB-200	0.578	0.258	hPB-350	0.785	0.377	dPB-440	0.580	0.186
dPB-200	0.476	0.177	dPB-350	0.717	0.281	dPB-440	0.379	0.088
hPB-200	0.381	0.070	hPB-350	0.613	0.266	dPB-440	0.189	0.032
hPB-200	0.187	0.023	hPB-350	0.397	0.108			
			hPB-350	0.205	0.030			

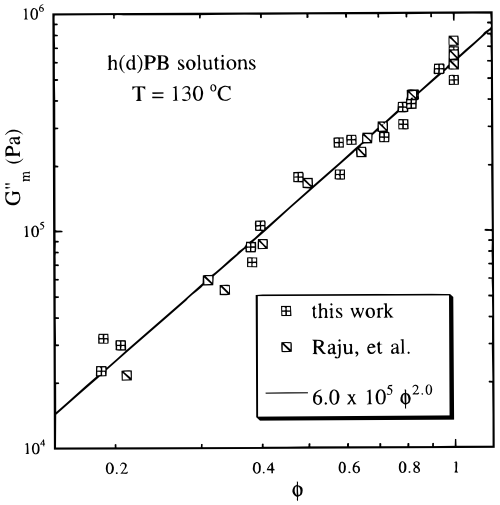

Figure 7. Data at 130 °C from the same solutions as in Figure 6, compared with results from Raju et al.;[26] the line indicates a global fit to a power law.

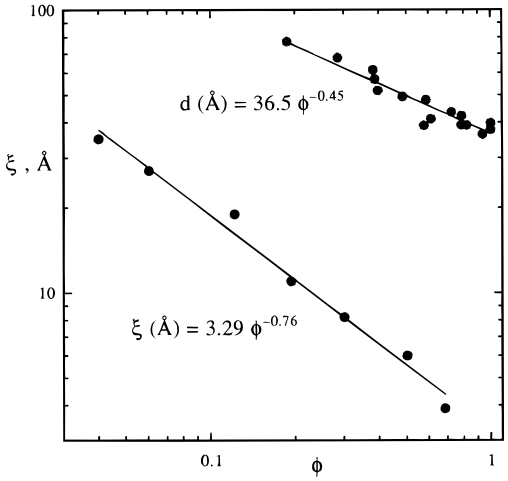

Figure 8. Comparison of the correlation length, ξ, and the entanglement spacing, d, as a function of concentration for hPB solutions.

The scaling approach relates the entanglement density to the chain contour per unit volume, with α an exponent to be determined experimentally.[32] The packing model equates the onset of entanglement effects to the chain molecular weight where the volume pervaded by the coil is exactly twice the volume occupied by the coil; the result corresponds to eq 6 with $\alpha = 3$.[19] Binary contact models attribute entanglements to a fixed number of binary contacts between chains, which corresponds to eq 6 with $\alpha = 2$. Colby and Rubinstein have modified this to a fixed number of binary contacts within an entanglement volume d^3, which leads to $\alpha = {}^9/_4$ in a good solvent and ${}^7/_3$ in a Θ solvent.[11] Topological models, such as those of Iwata and Edwards,[33] are mathematically more sophisticated but may not reduce to a unique value of α.

Experimentally, it is found that in solution the exponent α falls between 2 and 2.5, in clear disagreement with the packing model but consistent with the binary contacts/scaling approach. (However, it should be noted that in melts the packing model appears to describe the dependence of G_N and d on density and chain dimensions extremely well;[19] this discrepancy between solutions and melts is also an interesting unresolved issue.[31]) Our solution results fall on the end of the range obtained on other systems. Via neutron spin-echo measurements of hPB in $C_{19}D_{40}$, Richter et al. found $d \sim \phi^{-0.6}$ or $\alpha \approx 2.2$,[23] which apparently differs slightly from our result. Similarly, Raju et al. examined the rheological properties of hPB dissolved in low molecular weight polyethylene waxes at 130 °C and obtained $\alpha \approx 2.22$.[26] In Figure 7 we replot their data, along with those we obtained at 130 °C. Clearly, within the scatter of the data the two sets agree very well, particularly for $\phi \geq 0.4$. The differing exponents can be attributed to the small differences between the data sets at the lowest and highest concentrations. A global fit to all the data in Figure 7 gives an exponent of 2.0, as indicated by the line in Figure 7. Thus, these data underscore the potential difficulty in discriminating experimentally among exponents of 2, ${}^9/_4$, and ${}^7/_3$.

Comparison of Correlation Length and Entanglement Length. The polymer mode-coupling (PMC) theory of Schweizer and co-workers has emerged as a promising liquid-state approach to the dynamics of polymer liquids.[14−16] One particular issue that this model may be able to address is the apparent differing concentration dependences of the molecular weight exponents for the viscosity and the translational diffusion coefficient. Experimentally, one finds $\eta \sim M^{3.4\pm0.2}$ in both entangled melts and solutions, whereas $D \sim M^{-2}$ in polystyrene melts but $D \sim M^{-2.5}$ in entangled polystyrene solutions. Heretofore this difference has not been reconciled with the reptation model; note that the solution data extend up to 10^2 entanglements per chain and are therefore not easily attributed to the unentangled/entangled crossover. The PMC theory distinguishes between conformational (i.e., η) and center-of-mass (i.e., D) motion, and in particular the latter is dominated by relatively local frictional contributions. One consequence of this is that D is much more sensitive to the finite molecular weight effect dubbed "constraint porosity"[14,15] and is dependent on the parameter $\delta \equiv \xi/d$; η, in contrast, is predicted to be independent of δ. Qualitatively, constraint porosity may be viewed as reflecting fluctuations in the spatial distribution of entanglement constraints. Fuchs and Schweizer demonstrate that values of $\delta \leq 0.05$ are appropriate for melts,[15] which are sufficiently small that deviations from the asymptotic $D \sim M^{-2}$ are apparently not usually seen once M/M_e exceeds 5 or so. However, the larger exponents in solution, such as those reported by Nemoto and co-workers,[6−8] can be accommodated by $\delta \approx 0.3$.[15] The authors emphasize the importance of further stud-

ies of D and η in concentrated solutions and particularly in systems for which the relevant structural features (i.e., ξ and d) are also characterized. Accordingly, in Figure 8 the concentration dependence of ξ and d, and thus δ, is shown for hPB/*n*-alkanes. The values of d were obtained according to eqs 3 and 4 and utilizing $\langle h^2\rangle/M = 1.22$ Å^2 mol/g as obtained by Westermann et al.[25] The magnitude of δ increases from 0.09 in the melt to 0.15 by $\phi = 0.2$. Given the comparison of the PMC predictions with the polystyrene diffusion data of Nemoto et al.,[6−8] which implied a significantly larger change in δ with concentration, it might appear that this rather modest increase may not be sufficient to account for the diffusion exponents of ca. −2.5 observed in hPB solutions with $\phi = 0.20$ (to be presented subsequently[17]). However, our results in hPB melts,[17,18] combined with those in the literature, indicate that in fact the molecular weight exponent of D is closer to −2.3 than −2.0, and thus a smaller change in d between solutions and melts is anticipated.

Summary

The correlation length, ξ, has been determined for hPB as a function of concentration in a good solvent, $C_{16}D_{34}$, at 140 °C. The results for $\phi \geq 0.04$ follow the semidilute scaling prediction, $\xi \sim \phi^{-0.76}$, even up to polymer volume fractions as high as 0.7. The entanglement spacing, d, has been determined for hPB as a function of concentration in $C_{24}H_{50}$ at 140 °C, over the range from $0.2 \leq \phi \leq 1$, and is found to scale as $d \sim \phi^{-0.45}$. Thus, in this regime ξ and d may have different concentration dependences. The constraint porosity parameter, ξ/d, varies only modestly over this concentration range.

Acknowledgment. This work was supported by the National Science Foundation, through Grant DMR-9528481. We appreciate helpful discussions with R. H. Colby, W.W. Graessley, M. Rubinstein, and K.S. Schweizer and the willingness of L. J. Fetters to share the data on hPB coil dimensions in advance of publication. P. M. Cotts graciously provided SEC analysis of the polymers, and J. Schmidt performed most of the intrinsic viscosity measurements.

References and Notes

(1) de Gennes, P. G. *J. Chem. Phys.* **1971**, *55*, 572.
(2) de Gennes, P. G. *Scaling Concepts In Polymer Physics*; Cornell University Press: Ithaca, NY, 1979.
(3) Doi, M.; Edwards, S. F. *The Theory of Polymer Dynamics*, 2nd ed.; Clarendon Press: Oxford, 1988.
(4) Bueche, F. *J. Chem. Phys.* **1952**, *20*, 1959.
(5) Lodge, T. P.; Rotstein, N. A.; Prager, S. *Adv. Chem. Phys.* **1990**, *79*, 1.
(6) Nemoto, N.; Kishine, M.; Inoue, T.; Osaki, K. *Macromolecules* **1991**, *24*, 1648.
(7) Nemoto, N.; Kojima, T.; Inoue, T.; Kishine, M.; Hirayama, T.; Kurata, M. *Macromolecules* **1989**, *22*, 3793.
(8) Nemoto, N.; Kishine, M.; Inoue, T.; Osaki, K. *Macromolecules* **1990**, *23*, 659.
(9) Brown, W.; Nicolai, T. *Colloid Polym. Sci.* **1990**, *268*, 977.
(10) Koberstein, J. T.; Picot, C. *Polymer* **1986**, *27*, 1595.
(11) Colby, R. H.; Rubinstein, M. *Macromolecules* **1990**, *23*, 2753.
(12) Colby, R. H.; Rubinstein, M.; Daoud, M. *J. Phys. II (Paris)* **1994**, *4*, 1299.
(13) Colby, R. H. *J. Phys. II (Paris)* **1997**, *7*, 93.
(14) Fuchs, M.; Schweizer, K. S. *Macromolecules* **1997**, *30*, 5133.
(15) Fuchs, M.; Schweizer, K. S. *Macromolecules* **1997**, *30*, 5156.
(16) Schweizer, K. S.; Szamel, G. *Transport Theory Stat. Phys.* **1995**, *24*, 947.
(17) Tao, H.; Lodge, T. P.; von Meerwall, E. D., manuscript in preparation.
(18) Tao, H. Ph.D. Thesis, University of Minnesota, 1998.
(19) Fetters, L. J.; Lohse, D. J.; Richter, D.; Witten, T. A.; Zirkel, A. *Macromolecules* **1994**, *27*, 4639.
(20) Rosedale, J. H. Ph.D. Thesis, University of Minnesota, 1993.
(21) von Meerwall, E.; Beckman, S.; Jang, J.; Mattice, W. L. *J. Chem. Phys.* **1998**, *108*, 4299.
(22) Vrentas, J. S.; Venerus, P. C.; Vrentas, C. M. *Chem. Eng. Sci.* **1991**, *46*, 33.
(23) Richter, D.; Farago, B.; Butera, B.; Fetters, L. J.; Huang, J. S.; Ewen, B. *Macromolecules* **1993**, *26*, 795.
(24) Ferry, J. D. *Viscoelastic Properties of Polymers*, 3rd ed.; Wiley: New York, 1980.
(25) Westermann, S.; Richter, D.; Fetters, L. J., unpublished results.
(26) Raju, V. R.; Menezes, E. V.; Marin, G.; Graessley, W. W.; Fetters, L. J. *Macromolecules* **1981**, *14*, 1668.
(27) Kannan, R. M.; Lodge, T. P. *Macromolecules* **1997**, *30*, 3694.
(28) Jackson, J. K.; De Rosa, M. E.; Winter, H. H. *Macromolecules* **1994**, *27*, 2426.
(29) Flory, P. J.; Ciferri, A.; Chiang, R. *J. Am. Chem. Soc.* **1961**, *83*, 1023.
(30) Schaefer, D. W.; Joanny, J. F.; Pincus, P. *Macromolecules* **1980**, *13*, 1280.
(31) Raspaud, E.; Lairez, D.; Adam, M. *Macromolecules* **1995**, *28*, 927.
(32) Graessley, W. W.; Edwards, S. F. *Polymer* **1981**, *22*, 1329.
(33) Iwata, K.; Edwards, S. F. *J. Chem. Phys.* **1989**, *90*, 4567.

MA981468D